LA-UR - 98-2354

CONF-980605--

Los Alamos National Laboratory is operated by the University of California for the United States Department of Energy under contract W-7405 ENG-36

Title: MEASUREMENT AND SIMULATION OF APERTURES ON Z HOHLRAUMS

Author(s): Robert E. Chrien (P-22), Walter Matuska, Jr. (X-PA), Fritz J. Swenson (X-TA), Darrell L. Peterson (X-PA), Bernhard H. Wilde (X-TA), John L. Porter (Sandia), Stephen P. Breeze (Sandia), Larry E. Ruggles (Sandia), Walter W. Simpson(Sandia), Mark Vargas (Sandia).

Submitted to: Review of Scientific Instruments

DISCLAIMER

DISCLAIMER

Portions of this document may be illegible in electronic image products. Images are produced from the best available original document.

Measurement and simulation of apertures on Z hohlraums

R. E. Chrien, W. Matuska Jr., F. J. Swenson, D. L. Peterson, B. H. Wilde

Los Alamos National Laboratory, MS E526

Los Alamos, NM 87545

J. L. Porter, S. P. Breeze, L. E. Ruggles, W. W. Simpson, and M. Vargas

Sandia National Laboratory

Albuquerque, NM 87185-1187

(Presented on 19 June 1998)

Abstract

We have performed aperture measurements and simulations for vacuum hohlraums heated by wire array implosions. A low-Z plastic coating is often applied to the aperture to create a high ablation pressure which retards the expansion of the gold hohlraum wall. However this interface is unstable and may be subject to the development of highly nonlinear perturbations ("jets") as a result of shocks converging near the edge of the aperture. These experiments have been simulated using Lagrangian and Eulerian radiation hydrodynamics codes.

Typeset using REVTEX

I. INTRODUCTION

Aperture measurements are essential in determining the effective area through which the x-ray reemission flux from the wall of the hohlraum is transported as part of the hohlraum characterization in any high-temperature radiation environment. These measurements are equally important for understanding the coupling of energy out of vacuum hohlraums into a separate package for radiation diffusion or equation-of-state experiments. For example, this type of measurement has been widely used in laser-driven hohlraum experiments [1].

The 50 TW Z machine at Sandia is an array of 36 pulsed-power accelerators which efficiently implodes cylindrical wire array loads with masses of a few mg/cm by driving a current (up to 20 MA with a rise time of 100 ns) through the load in a z-pinch configuration [2]. We have used Z to drive loads consisting of 300 11–12 μm diameter tungsten wires arranged on a 20-mm diameter circle and contained within a gold-coated return current can of 24–26 mm diameter and 10–15 mm length which also serves as a vacuum hohlraum. The stagnation of the wires at the end of the implosion creates a high-temperature plasma which radiates $\simeq$ 50% of its kinetic energy in the form of x-rays (up to 2 MJ in a 6–7 ns FWHM pulse [2]). Simple estimates [1] indicate that a peak temperature of $\simeq$ 150 eV should be produced when this radiation is contained within the vacuum hohlraum. The hohlraum temperature predicted from a simulation of the wire array implosion is shown in Fig. 1.

Because the wires are also radiating during the implosion, there is a long ($\simeq$ 100 ns) foot on the radiation pulse which can lead to significant aperture closure prior to pinch stagnation. Thus it is necessary to design an aperture which will stay open as much as possible during the peak of the pulse. Furthermore, this radiation foot can create a subsonic radiation wave in a package designed to study supersonic radiation diffusion during the peak of the radiation pulse. A low-Z shield across the aperture is needed to absorb the foot of the pulse while attenuating the peak of the pulse as little as possible.

II. APERTURE MEASUREMENT TECHNIQUES

We have performed a series of aperture measurements on the Sandia Z facility using a pair of gated, filtered x-ray pinhole cameras. These cameras observe the x-ray reemission from one optical depth into the heated wall of the vacuum hohlraum. The albedo (ratio of reemitted and incident x-ray fluxes) is typically close to 0.9 near the time of peak hohlraum temperature [1]. Except for early times during the z-pinch implosion, the difference in reemission temperatures between the surface and one optical depth into the wall is only a few eV [1].

The Large-Format Pinhole Camera [4] (LFPC) uses nine vertical microchannel plate (MCP) strips, each 20-mm wide, 60-mm long, and 0.6-mm thick, with a microchannel length-to-diameter (L/D) ratio of 60, a optical width of 100 ps, and an impedance of 5.55 Ω. The LFPC has a magnification of 1.726 and uses one 100 μm diameter pinhole for each strip. It is filtered with 4.8 μm of kimfoil ($C_{16}H_{14}O_3$, 1.2 g/cm^3) plus 2.4 nm of Al and responds primarily to photons with energies between 255 and 281 eV (50% filter transmission). The point source resolution, estimated from the quadrature sum of geometric, diffractive, and MCP blurring, is 410 μm. The density-to-exposure correction for the film is determined using a calibrated step wedge.

The Filtered Pinhole Camera (FPC) uses four vertical 6-mm-wide MCP strips on a 40-mm diameter, 0.25-mm thick plate, with an L/D of 46, a optical gate width of 1 ns, and an impedance of 12.5 Ω. The FPC has a magnification of 0.98 and uses four pinholes for each strip, each with a separate diameter and x-ray filter. The filter material, energy range, pinhole diameter, and estimated resolution for each pinhole is shown in Table I. The density-to-exposure correction for the film is determined from measurements using a laser-produced x-ray source [3].

In all cases the LFPC and FPC viewed the apertures on the hohlraum at 12.5° above the horizontal midplane (77.5° from the axis). In order to view the wall reemission and avoid viewing the pinch, the aperture location was rotated by 20° or 40° about the hohlraum axis away from the line-of-sight.

The images from the LFPC and FPC are analyzed to determine the effective area of the aperture. In the analysis procedure, it is assumed that the maximum intensity I_{max} at the center of the image represents the unattenuated reemission flux from the hohlraum wall. Under this assumption, the effective area A_{eff} of the aperture is given by

$$A_{eff} = \int (I/I_{max})\, dA$$

where I is the intensity (exposure) of the image and the integral is performed over the area of the image. An equivalent expression is evaluated for the digitized image using a summation. If the maximum intensity in the image is attenuated by material blown-in from the aperture, then A_{eff} will overestimate the actual area. Likewise finite resolution will cause I_{max} to be reduced and A_{eff} will overestimate the actual area. Thus the above expression must be used with caution in situations with substantial aperture closure. The above caveats are taken into account in comparison with simulations of aperture closure by post-processing the results of the simulation using the same procedure as the data analysis and by folding the simulations with the diagnostic resolution.

III. APERTURE MEASUREMENTS

These experiments have tested a variety of aperture sizes, plastic tamper densities, and tamper thicknesses, as well as plastic window materials over the apertures to sharpen the radiation pulse on Z. The standard aperture geometry was a 2.4-mm diameter open hole in a 76-μm thick gold foil coated with 23.7 μm of parylene-n (CH, 1.12 g/cm^3). In other experiments, the aperture diameter was increased to 4 mm or the tamper thickness was increased to 60 μm. In a third type of experiment, an equivalent areal density of CH was applied but in the form of polystyrene foam. In the fourth type of experiment, a layer of solid density plastic or foam was applied across the aperture on the inside of the hohlraum.

An FPC image of a 4-mm diameter aperture tamped with 23.7 μm of CH and viewed at 40° hohlraum rotation is shown in Fig. 2. One observes that the image looks distinctly tilted. This tilted appearance suggests that the hohlraum wall has thickened as a result of gold blow-off. The effect is illustrated in a 3-D model of the aperture in a 1-mm-thick hohlraum wall as viewed by the FPC (Fig. 3).

The time history of A_{eff} for 2.4-mm diameter apertures tamped with 23.7 μm of CH is shown in Fig. 4. One observes that substantial reduction from the initial area of 4.52 mm^2 occurs during the foot of the radiation pulse. The variation in A_{eff} after the time of the pinch may be due in part to variations in the peak hohlraum temperature (115–145 eV) and in part to the breakdown in the analysis procedure for these large reductions in area.

IV. APERTURE SIMULATIONS

We have simulated the behavior of apertures on Z hohlraums using both Eulerian and Lagrangian codes. Magnetic fields were not included in either type of simulation. The advantage of Eulerian simulations of apertures is that regions which develop shear flows can be zoned more finely in those regions without tangling the mesh. Also fixed, fine zones in the Eulerian grid better resolve the temperature and density gradients across the aperture which is important when calculating the aperture area. The Eulerian simulations were performed using a code employing fixed rectangular zones and a one-temperature radiation diffusion model. Images were then calculated based on these simulations using the reemission spectrum from the inside of the hohlraum, as well as absorption and reemission due to the aperture materials. The viewing angle and the detector response were also included. These images were then processed to generate effective areas using the same procedure used to process the image data. The time history of the area from the Eulerian simulations is shown in Fig. 4. The simulations are in reasonable agreement with the data, except for the latest times when the aperture area is reduced to less than half of the initial area.

Density contours from the Eulerian simulations show a "jet" developing at the inner edge of the aperture (Fig. 5). The jet is thought to be caused by the interaction of shocks developed in the plastic tamping on the edges of the gold aperture surfaces. The evolution of the jet is calculated to depend only weakly on the shape of the edges of the aperture. The inward motion of the jet may contribute to the apparent thickening of the wall leading to the tilted appearance of the images. However, more detailed spatially-resolved measurements are needed to determine whether the jet appearing in the simulations is real.

We have also performed some simulations with the Lagrangian code LASNEX [5]. These preliminary calculations using coarse zoning show different aperture behavior than the Eulerian calculations, with no indication of jetting. Many if not all of the differences are likely due to the zoning, but calculations with finer zoning have not yet been performed. Such finely zoned calculations are required in order to ascertain any intrinsic differences between Eulerian and Lagrangian methods. However, if zoning of similar scale size as that used in the Eulerian calculations is required to resolve a jet from the edge of the aperture, then a satisfactory comparison between Lagrangian and Eulerian codes may be very difficult. Newer "arbitrary Lagrangian-Eulerian" and "free Lagrange" codes may also be useful in simulations of aperture behavior since they calculate shear flow without tangling the mesh.

V. DISCUSSION

We are pursuing a number of directions in our study of apertures on Z hohlraums. These experiments would clearly benefit from improvements in diagnostic resolution through the use of Kirkpatrick-Baez imaging systems in place of remotely-placed pinholes. Spatial resolution on the order of 10 μm should be possible. We are exploring the use of thicker tamping layers to delay the shock interactions thought to lead to the jetting phenomenon. The strength of the shocks might also be affected by the density of the tamping layer, so we are pursuing the use of foam layers instead of parylene-n coatings. We are also exploring the effect of burn thru foils placed across the inside of the aperture as a way of filling the aperture with material which will retard the blow-in of the gold but which will be fully ionized at the peak of the radiation pulse.

ACKNOWLEDGMENT

This work was supported by US DOE contracts W-7405-ENG-36 and DE-AC04-76-DP00789.

REFERENCES

[1] John Lindl, Phys. Plasmas **2**, 3933 (1995).

[2] R. B. Spielman, et al., Phys. Plasmas **5**, 2105 (1998).

[3] L. E. Ruggles, et al., these proceedings.

[4] L. E. Ruggles, et al., Rev. Sci. Instrum. **66**, 712 (1995).

[5] G. Zimmerman, W. Kruer, Comments Plasma Phys. Controlled Fusion **11**, 51 (1975).

FIGURES

FIG. 1. 2-D radiation magnetohydrodynamic simulation of the radiation temperature in the vacuum hohlraum driven by the wire array implosion.

FIG. 2. FPC image of 4-mm-diameter aperture tamped with 23.7 μm of CH.

FIG. 3. 3-D model of 4-mm-diameter aperture in a 1-mm-thick hohlraum wall as viewed by the FPC.

FIG. 4. Time history of A_{eff} for 2.4-mm diameter apertures tamped with 23.7 μm of CH, together with post-processed areas from Eulerian simulations.

FIG. 5. Density profile from the Eulerian simulation of an aperture showing a "jet" of gold blow-off emerging from the edge of the aperture. The interior of the hohlraum is toward the left.

TABLES

TABLE I. Filters and pinholes for the FPC.

filter	thickness (μm)	photon energy (eV)	pinhole diameter (μm)	resolution (μm)
boron	2	158–184	200	530
parylene-n (Al)	5 (.1)	255–281	150	435
titanium	1	374–455	250	577
chromium	1	489–563	250	553

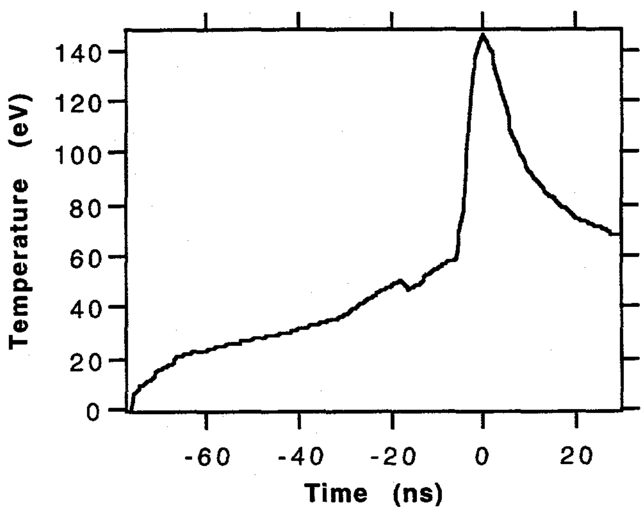

Figure 1

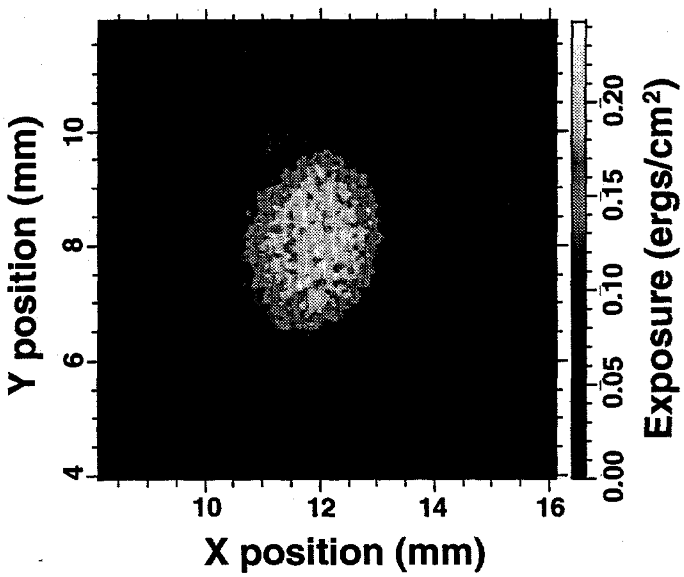
Y position (mm)
4
6
8
10
X position (mm)
10
12
14
16
Exposure (ergs/cm^2)
0.00
0.05
0.10
0.15
0.20

Figure 2

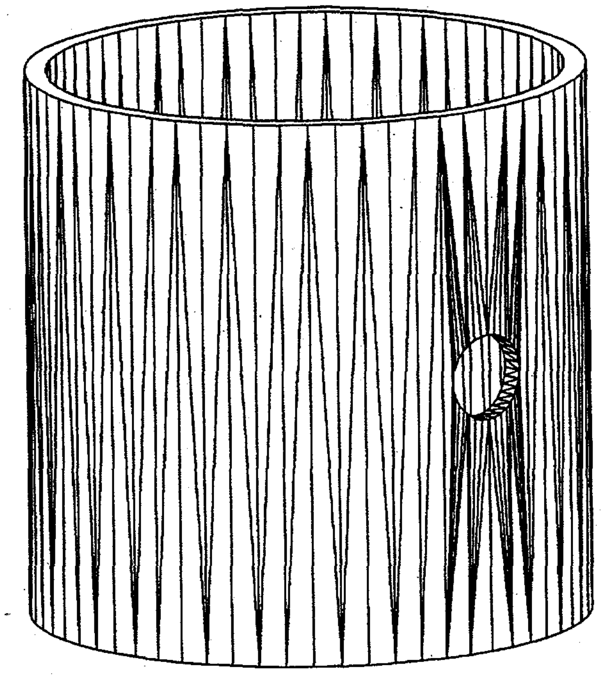

Figure 3

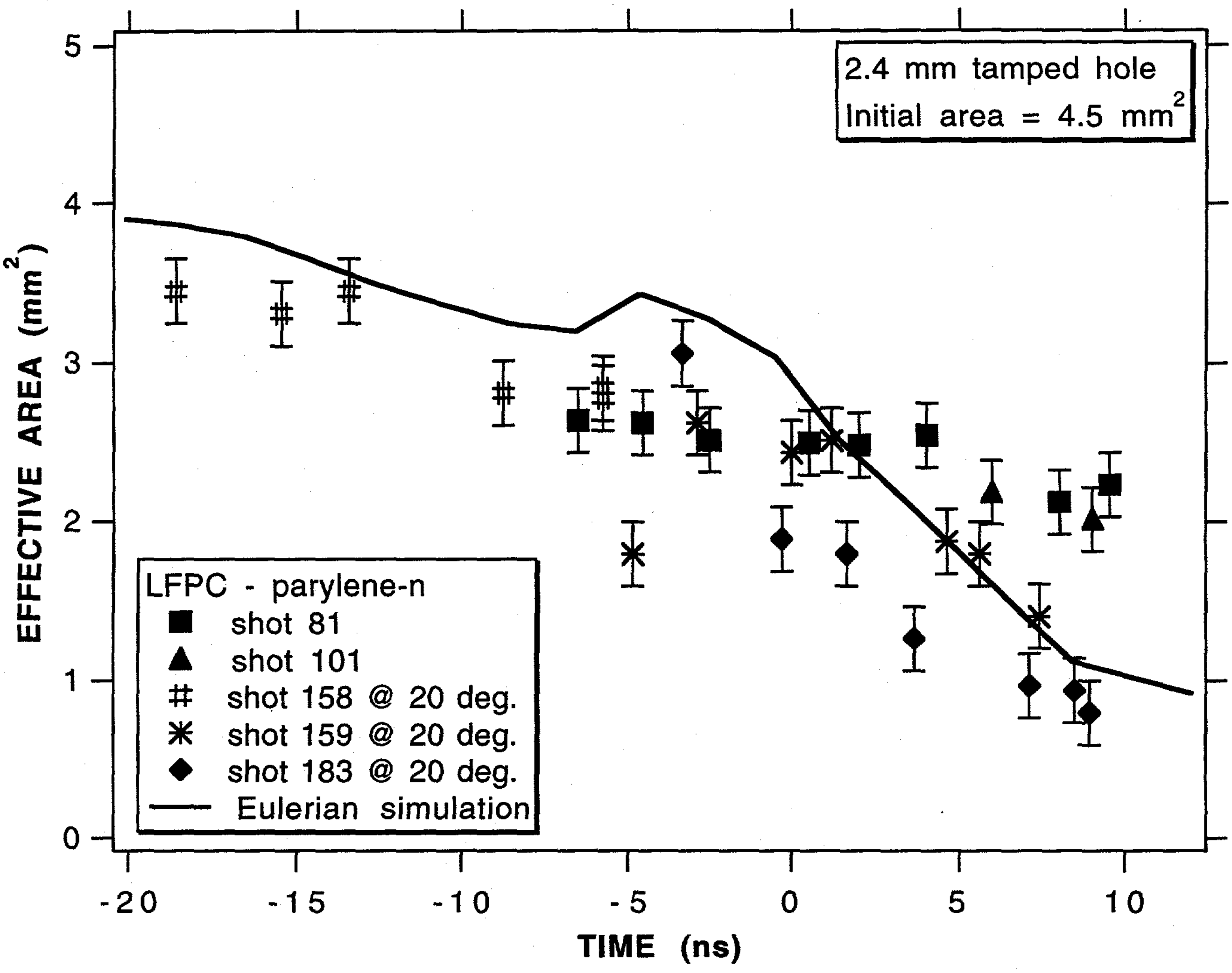
2.4 mm tamped hole
Initial area = 4.5 mm^2
LFPC - parylene-n
shot 81
shot 101
shot 158 @ 20 deg.
shot 159 @ 20 deg.
shot 183 @ 20 deg.
Eulerian simulation
EFFECTIVE AREA (mm^2)
TIME (ns)
0
1
2
3
4
5
-20
-15
-10
-5
0
5
10

Figure 4

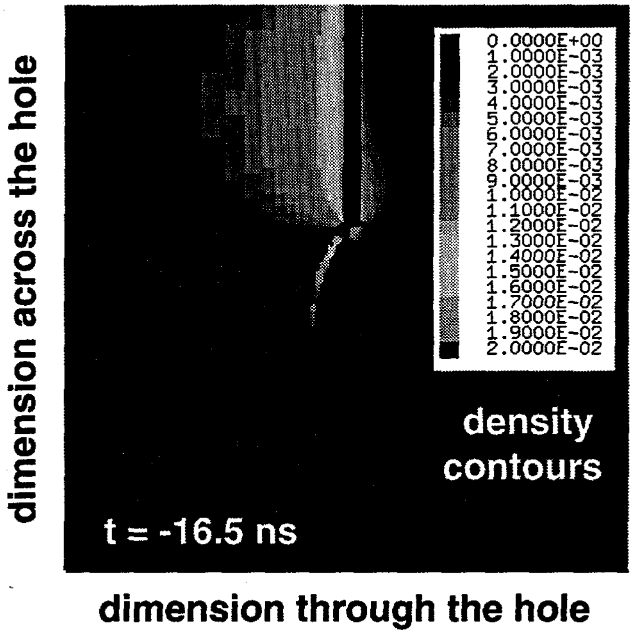
dimension across the hole
0.0000E+00
1.0000E-03
2.0000E-03
3.0000E-03
4.0000E-03
5.0000E-03
6.0000E-03
7.0000E-03
8.0000E-03
9.0000E-03
1.0000E-02
1.1000E-02
1.2000E-02
1.3000E-02
1.4000E-02
1.5000E-02
1.6000E-02
1.7000E-02
1.8000E-02
1.9000E-02
2.0000E-02
density contours
t = -16.5 ns
dimension through the hole

Figure 5